

Quantum Confinement of Hot Image-Potential State Electrons

K. Schouteden* and C. Van Haesendonck

Laboratory of Solid-State Physics and Magnetism and Institute for Nanoscale Physics and Chemistry (INPAC),
BE-3001 Leuven, Belgium

(Received 14 August 2009; published 28 December 2009)

Discrete image-potential state (IS) resonances at Co nanoislands on Au(111) are probed using scanning tunneling microscopy and spectroscopy. We observe particle-in-box-type standing wave patterns, which is surprising in view of the high energy of the IS electrons when compared to the confining potential imposed by the island edges. The weak confining potential experienced by the IS electrons results in electronic interaction effects between closely spaced islands. Probing high-energy ISs hence provides a novel route to investigate electronic coupling between nanoislands on surfaces.

DOI: 10.1103/PhysRevLett.103.266805

PACS numbers: 73.22.-f, 68.37.Ef, 73.20.At

Image-potential states provide an ideal playground for investigation of fundamental physical properties such as the dynamics of excited surface electrons. Image-potential state (IS) electrons are confined along the surface normal by the crystal surface potential at one side and by the Coulomblike image potential at the vacuum side [1,2]. This results in the formation of hydrogenlike states, in which electrons act as a two-dimensional (2D) free-electron-like gas that can move freely along the surface [3]. The interaction of IS electrons with underlying bulk state electrons causes the ISs to broaden into resonances. This interaction has been studied intensively by means of two-photon photoemission spectroscopy (2PPE), yielding valuable information about the dynamics and lifetime of IS electrons [3,4], as well as about the influence of insulating top layers [5] and of nanostructuring [6] on the work function of metallic surfaces.

Whereas 2PPE experiments provide area-averaged information, scanning tunneling microscopy (STM) and scanning tunneling spectroscopy (STS) allow local investigation of IS phenomena with high spatial and energy resolution. Soon after the invention of the scanning tunneling microscope, STM and STS in the distance-voltage $z(V)$ spectroscopy mode were introduced to study ISs at surfaces [7]. In this mode the tunneling voltage V is ramped while the tunneling current I is kept constant by increasing the distance z of the STM tip to the substrate as more and more (image-potential) states become available for tunneling. Figure 1 presents a schematic energy diagram of an STM tip in close vicinity of a metal surface. Because of the applied electric field between STM tip and sample, the ISs shift to higher energies and their energy spacings expand. It has been demonstrated that tunneling via ISs allows detailed visualization of the surface of insulating diamond films with atomic resolution [8]. IS dynamics has recently been investigated for various flat surfaces, including Fe [9], Au [10] and Cu surfaces [10,11]. While the idea has been put forward before [11,12], experimental observation of ISs confined at nanosize metallic particles is still lacking.

To the best of our knowledge, so far only circularly shaped Na nanoislands on Cu(111) surfaces have been studied theoretically [12].

In this Letter we report on a detailed experimental study of ISs at nanoscale Co islands using STM and STS $z(V)$ -grid measurements. Up to five ISs are resolved within the investigated energy range. The energy of these confined ISs depends on the island size. In spite of the high energy of the electrons and the fact that they move at a distance of the order of 1 nm above the surface [2], scattering of the IS electrons at the island edges surprisingly gives rise to the formation of particle-in-box-type standing wave patterns in dz/dV maps. The patterns are observed to “spill out” of the nanoscale island at high energies. This way, probing the high-energy ISs provides a novel route to investigate electronic interactions between closely spaced metallic nanoislands on surfaces, thereby offering clear challenges related to understanding the confinement of and the spatial coupling between image-potential states.

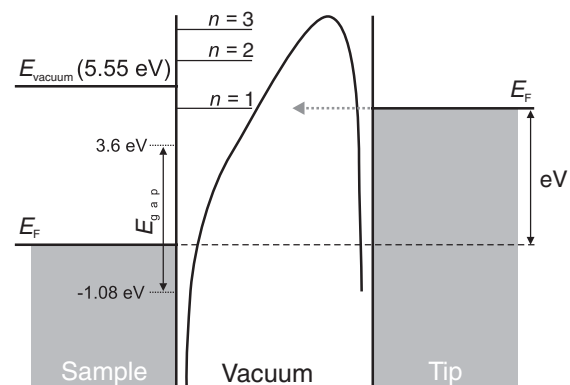


FIG. 1. Schematic energy diagram of an STM tip in tunnel contact with a Au(111) surface at voltage V . The Au(111) surface exhibits a gap E_{gap} in its projected bulk band structure. Image-potential states exist at elevated energies near the vacuum level E_{vacuum} . Indicated energies are with respect to the Fermi level E_F and are taken from Ref. [19].

Atomically flat Au(111) films are epitaxially grown *ex situ* on mica and are cleaned *in situ* in the preparation chamber of our ultra high vacuum STM setup by sputtering and annealing cycles, after which Co atoms are deposited at room temperature as described in Ref. [13]. Deposited Co atoms self-organize into bilayer islands of only a few nanometers in size (1 ML of Co(0001) = 0.205 nm) [14]. STM and STS measurements are performed with a low-temperature STM (Omicron Nanotechnology), operating at a base pressure in the 10^{-11} mbar range ($T_{\text{sample}} \approx 4.5$ K). Electrochemically etched W tips are cleaned *in situ* by repeated flashing well above 1000 K to remove the surface oxide layer and additional contamination. STM topographic imaging is performed in constant current mode. $z(V)$ curves are recorded with closed feedback loop with a grid size of 200×200 points, from which $dz/dV(V)$ curves are obtained numerically and color maps that directly reflect the local density of states (LDOS) [9,15] (referred to as dz/dV maps hereafter) can be produced at selected values of the tunneling voltage V . The tunneling voltages indicated in the text and figure captions are with respect to the sample, while the STM tip is virtually grounded. Image processing was performed by Nanotec WSXM [16].

In Fig. 2(a) we present an STM topography image of a Co island on Au(111) with the shape of a truncated triangle, recorded simultaneously during a $z(V)$ -grid measurement. A typical Co island $dz/dV(V)$ spectrum, taken at

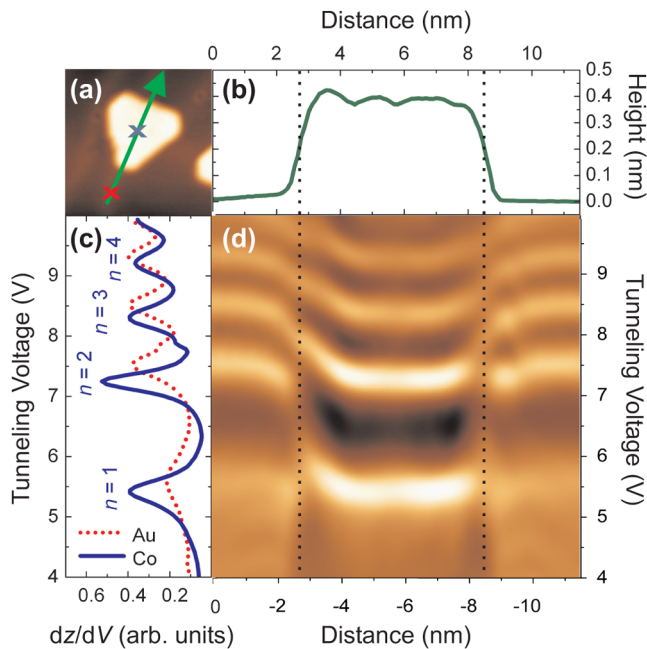


FIG. 2 (color online). (a) $12 \times 12 \text{ nm}^2$ STM image of a Co island with the shape of a truncated triangle. (b) Height profile along the green arrow in (a). (c) $dz/dV(V)$ spectrum at the center of the Co island (blue cross) and at the surrounding Au(111) surface (red cross). (d) 2D visualization of the $dz/dV(V)$ spectra along the green arrow in (a) ($I = 10.0 \text{ nA}$, $V = 2.0 \text{ V}$).

the blue cross in Fig. 2(a), is plotted in Fig. 2(c), revealing the existence of discrete ISs at the nanoscale Co island. A curve obtained at the surrounding Au(111) surface is added as a reference. The Co island ISs appear at different energies than for the flat Au(111) surface. On the other hand, the Co island IS maxima are more pronounced when compared to the Au(111) surface, which can be linked to the confinement of the IS electrons to the nanoisland [17] and a weaker coupling of the ISs to the Au bulk state electrons. In Fig. 2(d) we present a 2D visualization of the $dz/dV(V)$ spectra along the green arrow in Fig. 2(a). The ISs maxima in Fig. 2(c) appear as bright maxima in Fig. 2(d). Surprisingly, the 2D visualization reveals that there occurs a gradual transition from the n Co IS maxima to the $n + 1$ Au(111) maxima. Although less pronounced, a somewhat similar crossover between ISs with different n value has recently been observed for the ISs of insulating NaCl islands and the underlying Ag(100) surface (see Fig. 5 in Ref. [5]), while such a crossover was not observed for nanostructured Pt(111) surfaces covered with two monolayers of Ag (see Fig. 2 in Ref. [6]). When carefully comparing Figs. 2(b) and 2(d), it can be observed that this transition is completed somewhat outside of the Co island, in particular, for the $n = 3$ Co IS. On one hand, due to the finite size of the tip, extrinsic smearing effects (convolution effects) will be present [5]. On the other hand, taking into account the very small size of the Co island and the finite height of the potential barrier created by the island edges [12,17,18] for the high-energy IS electrons, an intrinsic spill out of the island electronic wave functions as well as a “penetration” of the Au(111) IS electrons into the Co island can be expected. As discussed in more detail below, this implies that the ISs electrons of closely spaced metal-

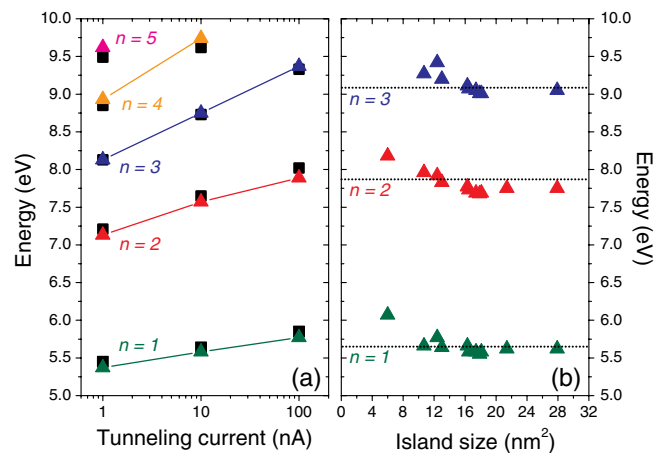


FIG. 3 (color online). (a) Influence of the applied tunneling current on the energy of ISs at an isolated Co island (colored triangles) and at the Au(111) surface (black squares) ($V = 2.0 \text{ V}$). The colored lines are only a guide to the eye. (b) Dependence of the energy of the ISs with $n = 1-3$ on the Co island size. Black dotted lines indicate the Au ISs ($I = 10.0 \text{ nA}$, $V = 2.0 \text{ V}$).

lic nanoparticles on a metallic surface are able to interact with each other and this interaction can be probed directly by $z(V)$ STS measurements.

In Fig. 3(a) we present the dependence of the Co (colored triangles) and Au (black squares) IS maxima on the applied tunneling current for an isolated Co island. The Co ISs experience a Stark shift to higher energies, similar to the Au ISs [10]. This shift becomes more pronounced with increasing IS number n . There also occurs a crossover: With increasing n the Co IS maxima move from slightly below to above the corresponding maxima of the Au(111) surface. The crossover depends on the size of the Co island, which can be linked to the dependence of the energy of the Co island ISs on the size of the probed nanoisland. This is illustrated in Fig. 3(b) (colored triangles), where the Au IS maxima have been added as a reference (black dotted lines). The Co IS maxima increase from slightly below to above the corresponding maxima of the Au surface with decreasing island size, i.e., with increasing lateral confinement of the IS electrons to the nanoisland [17]. Finally, it should be noted that all data in Figs. 3(a) and 3(b) are obtained with the same STM tip. It is known that the precise energy of the IS maxima depends on the tip geometry [10].

In Figs. 4(a)–4(i) we present a topographic STM image [(a)] of the same Co island as the one in Fig. 2(a), together with a series of dz/dV maps [(b)–(i)] at the indicated

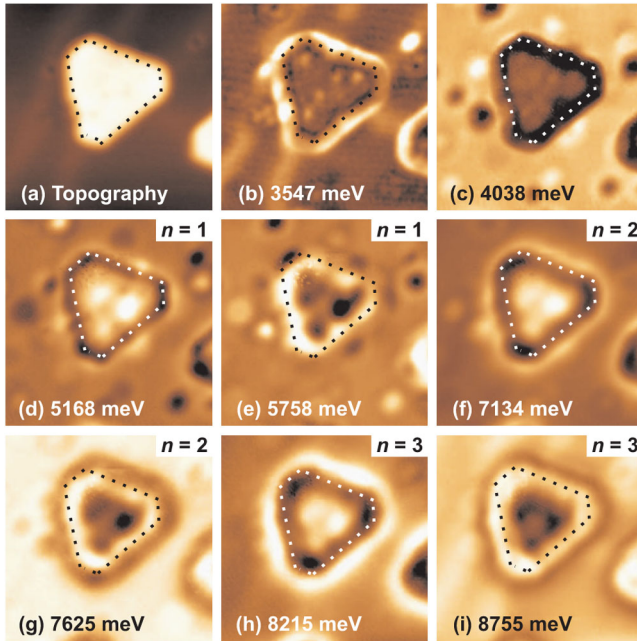


FIG. 4 (color online). (a) $12 \times 12 \text{ nm}^2$ STM topography image of a Co island on Au(111). (b)–(i) dz/dV maps at the indicated tunneling voltages, revealing standing wave patterns that are formed due to confinement of IS electrons by the edges of the Co island. The topographic contour of the Co island has been added for ease of comparison as a white/black dotted truncated triangle ($I = 10.0 \text{ nA}$, $V = 2.0 \text{ V}$).

tunneling voltages. The dotted lines indicate the contours of the Co island determined from Fig. 4(a). Labels indicate the IS number n to which the dz/dV maps correspond [also see Fig. 2(c)]. Up to energies of around 3.7 eV, previously investigated standing wave patterns of scattered surface state electrons can be resolved within the island interior as well as on the Au(111) surface [Fig. 4(b)] [13]. This energy value coincides fairly well with the top of the projected bulk band gap for the Au(111) surface (see Fig. 1) in which the Au(111) surface state band is located [19]. No pronounced features are observed in the dz/dV maps up to around 5 eV [Fig. 4(c)], which is around the Au(111) vacuum level E_{vacuum} (see Fig. 1) [19]. Above this energy patterns are resolved that reflect the shape and the threefold symmetry of the Co island. We assign these patterns to interference of the 2D free-electron-like IS electrons that are scattered at the potential barrier induced by the Co island edges. In Figs. 4(d) and 4(e) we present the two most pronounced patterns that can be resolved within the Co $n = 1$ IS band. Remarkably, the patterns observed for the Co $n = 1$ IS band are retrieved as well for the Co $n = 2$ [Figs. 4(f) and 4(g)] and the Co $n = 3$ [Figs. 4(h) and 4(i)] IS bands. These patterns are consistent with previous particle-in-a-box based LDOS calculations of the second and the third eigenstate of a box having the same shape and symmetry as the island in Fig. 4 [13,18]. This confirms that the IS related standing wave patterns reflect a particle-in-box-type behavior. Each IS n is described in terms of a band with different onset energy E_0 , which is located near the LDOS maximum of the corresponding IS, according to

$$E_n = E_0 + \frac{\lambda_n}{m^* \Omega}, \quad n = 1, 2, 3, \dots, \quad (1)$$

where Ω denotes the island surface area, $m^* \approx 1$ [3] is the electron effective mass (of the 2D free-electron-like IS electrons) and the λ_n are the eigenvalues of the box. As indicated above, confinement of IS electrons has been addressed theoretically by Borisov *et al.* for circular Na islands on Cu(111) surfaces [12]. According to Borisov *et al.*, spatially confined ISs develop at metal-supported metallic nanoislands provided (i) the work function of the island is lower than that of the substrate and (ii) there is a band gap in the projected bulk band structure. Here, both conditions are fulfilled, since Au(111) has a gap in the projected band structure (see Fig. 1) and the work function of Co(0001) ($\approx 5.20 \text{ eV}$ [20]) is lower than that of Au(111) ($\approx 5.55 \text{ eV}$ [19]).

From the indicated contours (dotted lines) in the dz/dV maps it becomes clear that the electronic features at the Co island site exceed the size of the Co island inferred from the topographic image in Fig. 4(a), especially at the highest energies [see, e.g., Fig. 4(i)]. Keeping in mind the small size of the Co island, this observation may be related to spill out of high-energy IS electrons, as already mentioned above. This indicates that electronic interaction via high-

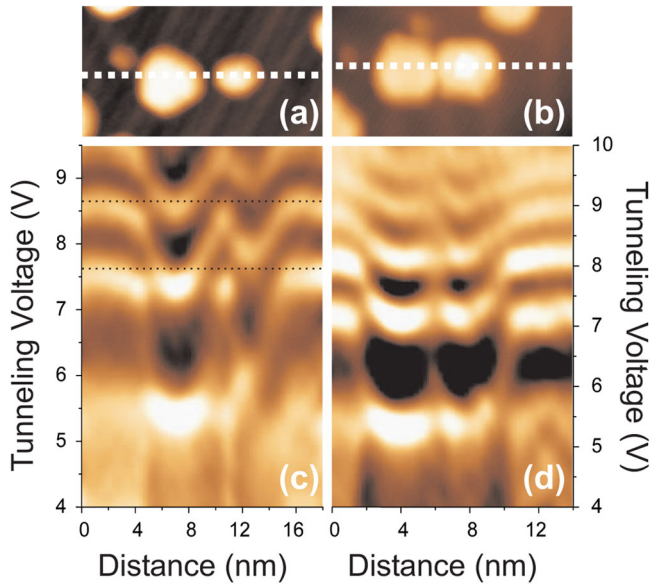


FIG. 5 (color online). (a) $18 \times 10 \text{ nm}^2$ and (b) $14 \times 9 \text{ nm}^2$ STM topography image of two Co islands in close proximity ($I = 1.0 \text{ nA}$, $V = 2.0 \text{ V}$). (c) and (d) 2D visualization of the $dz/dV(V)$ spectra along the white dotted line in (a) and (b), respectively. Black dotted lines in (c) correspond to the $n = 2$ (lower dotted line) and $n = 3$ (upper dotted line) ISs of the bare Au(111) surface ($I = 1.0 \text{ nA}$, $V = 2.0 \text{ V}$).

energy ISs between closely spaced Co islands should be taken into account. In Figs. 5(a) and 5(b) we present topographic STM images of two sets of closely spaced Co islands, while in Figs. 5(c) and 5(d) we present a 2D visualization of the $dz/dV(V)$ spectra along the white dotted line in (a) and (b), respectively. Since for each set of islands a different STM tip has been used, a different number of ISs with different energy spacings is accessible [10]. Similar to the case of the Co island in Fig. 2, we surprisingly find that the n Co IS maxima evolve into the $n + 1$ Au(111) maxima outside of the Co islands. On the other hand, the IS maxima of the bare Au(111) surface are not retrieved in between the two Co islands, which can be related to the intrinsic spatial broadening of the high-energy Co IS wave functions [2]. In addition, the transition between the Co islands and the bare Au(111) surface becomes considerably smoother for ISs with higher n [see Figs. 5(c) and 5(d), as well as Fig. 2(d)] and may be related to the spillout of high-energy IS electrons. This is consistent with recently reported results by Borisov *et al.* for circularly shaped Na nanoislands on Cu(111) surfaces based on combined density functional theory calculations and time-dependent wave packet propagation [12]. Related calculations, with the additional complication of a less symmetric confinement potential, will be needed to achieve a quantitative description of our experimental results. In order to reproduce the surprising experimental

fact that the n Co IS maxima evolve into the $n + 1$ Au(111) maxima outside of the Co islands (see Figs. 2 and 5), it may be necessary to take into account the specific electric field distribution at the Co island edges that depends on the STM tip geometry.

In conclusion, we have successfully probed spatial confinement of image-potential states at nanoscale metallic Co islands on a Au(111) surface by means of STM and STS in the $z(V)$ spectroscopy mode. The confinement results in a size-dependence of the energy of these states. In spite of the fact that the high-energy IS electrons move well above the surface, scattering of image-potential state electrons at the island edges results in the formation of particle-in-box-type standing wave patterns. The wave function of the islands is observed to spill out of the islands, which may be related to the high electron energy and the very small size of the island. This way, our $z(V)$ -grid measurements allow us to investigate the electronic interaction between neighboring nanoislands that are separated by a distance of the order of 1 nm.

This work has been supported by the Fund for Scientific Research—Flanders (FWO, Belgium) as well as by the Belgian Interuniversity Attraction Poles (IAP) and the Flemish Concerted Action (GOA) research programs.

*Koen.Schouteden@fys.kuleuven.be

- [1] P.M. Echenique and J.B. Pendry, *J. Phys. C* **11**, 2065 (1978).
- [2] E. V. Chulkov, V.M. Silkin, and P.M. Echenique, *Surf. Sci.* **437**, 330 (1999).
- [3] M. Weinelt, *J. Phys. Condens. Matter* **14**, R1099 (2002).
- [4] S. Schuppler *et al.*, *Phys. Rev. B* **46**, 13 539 (1992).
- [5] H.-C. Ploigt *et al.*, *Phys. Rev. B* **76**, 195404 (2007).
- [6] P. Ruffieux *et al.*, *Phys. Rev. Lett.* **102**, 086807 (2009).
- [7] G. Binnig *et al.*, *Phys. Rev. Lett.* **55**, 991 (1985).
- [8] K. Bobrov, A.J. Mayne, and G. Dujardin, *Nature (London)* **413**, 616 (2001).
- [9] A. Kubetzka, M. Bode, and R. Wiesendanger, *Appl. Phys. Lett.* **91**, 012508 (2007).
- [10] D.B. Dougherty *et al.*, *Phys. Rev. B* **76**, 125428 (2007).
- [11] P. Wahl *et al.*, *Phys. Rev. Lett.* **91**, 106802 (2003).
- [12] A.G. Borisov *et al.*, *Phys. Rev. B* **76**, 121402 (2007).
- [13] K. Schouteden *et al.*, *New J. Phys.* **10**, 043016 (2008).
- [14] B. Voigtländer, G. Meyer, and N.M. Amer, *Phys. Rev. B* **44**, 10 354 (1991).
- [15] N. Garcia, *IBM J. Res. Dev.* **30**, 533 (1986).
- [16] I. Horcas *et al.*, *Rev. Sci. Instrum.* **78**, 013705 (2007).
- [17] J. Li *et al.*, *Phys. Rev. Lett.* **80**, 3332 (1998).
- [18] E. Lijnen, L.F. Chibotaru, and A. Ceulemans, *Phys. Rev. E* **77**, 016702 (2008).
- [19] E. V. Chulkov, M. Machado, and V.M. Silkin, *Vacuum* **61**, 95 (2001).
- [20] R. Fischer *et al.*, *Phys. Rev. B* **46**, 9691 (1992).